

Ductile Connections in Precast Concrete Moment Resisting Frames



Onur Ertas

Research Assistant
Department of Civil Engineering
Bogazici University
Bebek, Istanbul, Turkey

Sevket Ozden

Assistant Professor
Department of Civil Engineering
Kocaeli University
Kocaeli, Turkey



Turan Ozturan

Professor
Department of Civil Engineering
Bogazici University
Bebek, Istanbul, Turkey

This paper presents the test results of four types of ductile, moment-resisting precast concrete frame connections and one monolithic concrete connection, all designed for use in high seismic zones. The performance of the precast concrete connections subject to displacement control reversed cyclic loading is compared with that of the monolithic connection. The precast concrete connections tested may be subdivided into three groups, namely cast-in-place, composite with welding, and bolted. The cast-in-place connections were located in either the beam or the column of the precast concrete subassemblies. The composite connection is a common detail used in the Turkish precast concrete industry. Two bolted specimens without corbels were also tested. Through these tests, the responses of different connection types under the same loading pattern and test configuration were compared. Comparisons of performance parameters, such as energy dissipation and ease of fabrication, revealed that the modified bolted connection may be suitable for use in high seismic zones.

Precast concrete provides high-quality structural elements, construction efficiency, and savings in time and overall cost of investment. In order to validate these benefits, and to expand the market for precast concrete structures in seismic regions, the performance and capacity

of specially designed connections were evaluated. Many precast concrete structures were heavily damaged by the recent earthquakes (Adana–Ceyhan in 1997 and Koaceli and Duzce in 1999) that hit the industrial heartland of Turkey, and the poor performance of their connections may be the primary reason for the widespread damage.

As a result, a two-phase research program on the performance of ductile beam–column connections of precast concrete was developed in the Bogazici and Kocaeli Universities after the 1999 earthquakes. This program was funded by the Scientific and Technical Research Council of Turkey (TUBITAK) (Project No: ICTAG I589) and the Turkish Precast Concrete Association. In Phase I of the research program, cast-in-place, composite, and bolted connections were investigated and compared with a monolithic connection counterpart. The Phase I connection types were chosen from the most widely used types according to construction practices in North America, Europe, and Japan. In Phase II, post-tensioned hybrid connections with different mild steel reinforcement ratios were examined. Only Phase I test results and proposed recommendations are presented in this paper. Performance comparisons are made according to strength predictions, stiffness degradation, and energy dissipation of the connections. All test specimens in this research program are detailed according to the governing building codes or the available literature.

LITERATURE SURVEY

The detailing and location of precast concrete connections has been the subject of numerous experimental and analytical investigations. In the study by Restrepo et al.,¹ six different cast-in-place (CIP) connection details with different reinforcement configurations and connection locations were studied. Specimen Unit 5 in Restrepo's research consisted of precast concrete beams placed between columns and a CIP concrete joint core that was constructed between the beam-joining ends. The beams were seated 1.2 in. (30 mm) into the column gap, and the test results revealed that there was no need for special detailing at the vertical cold joints, such as shear keys. Alcocer et al., Rodriguez, and Blandon also performed some CIP connection tests.^{2–4} They reported that plastic hinging developed at the column face. Although the type of connection tested did not fully emulate monolithic construction, it is reported that this type of connection can be used with precast concrete frame systems or in hybrid systems, provided that the strength and stiffness of the system are taken into account.

The use of steel fiber–reinforced concrete in the CIP connections was reported to be very effective in improving the displacement ductility and energy dissipation of the specimens and in leading to slower stiffness degradation. The addition of steel fibers also improves the bond strength of the reinforcing bars within the connection region.^{5,6}

Bhatt et al and Seckin et al developed some welded connections for use in precast concrete structures.^{7,8} Although the behavior of the connections under consideration was satisfactory, the construction of these specimens requires significant

welding of the beam and column reinforcement. The cost and quality-control measures associated with excessive welding may offset some inherent advantages of the precast concrete construction if applied in the field. Moreover, the heat generated from welding may cause damage to the bond of steel bars and result in cracking of the adjacent precast concrete. Therefore, field welding needs to be minimized in precast concrete construction.^{9–11}

Bolted connections, or ductile links, where the precast concrete beams are connected directly to the column faces in precast concrete structures, may be the most cost-effective construction practice. In these types of connections, the friction force created by the flexural moment resists the vertical shear at the beam–column interfaces.¹² French et al presented the response of various types of beam–column connections; some of the connections developed plastic hinges outside the connection region.^{13,14} French's research revealed that the threaded reinforcing bar connections with tapered, threaded splices proved to be the most favorable solution in terms of performance, fabrication, and economy. In the PRESSS Program, similar connection details, called tension-compression yield (TCY) connections, with mild steel were tested, and the performance of TCY connections was reported to be similar to that of monolithic specimens. The disadvantage of the TCY system may be the high residual displacement and the low residual stiffness after inelastic seismic response.¹⁵

Ghosh et al presented a paper about a strong connection concept developed with the 1997 International Conferences of Building Officials' *Uniform Building Code: V. 2, Structural Engineering Design Provisions* for precast concrete structures located in high seismic zones.^{16,17} A strong connection is designed to remain elastic while inelastic action takes place away from the connection. Because a strong connection must not yield or slip, its design strength in both flexure and shear must be greater than the bending moment and shear force, respectively, corresponding to the probable flexural or shear strengths at the nonlinear action location.¹⁸ In addition to the greater cost of strong connections, the overstrength required in the connectors becomes quite large as the hinge location is moved away from the column face. Also, the hinge relocation approach, where the hinge is relocated away from the column face, increases the rotational ductility demand of the probable hinge for a given story drift. It should be noted that satisfactory seismic performance requires an overall system that is able to sustain large lateral deformations without significant loss of strength.¹⁹

TEST SPECIMEN AND CONNECTION DETAILS

Phase I test specimens were modeled as exterior joints of a multistory building. They were designed according to the strong column and weak beam design philosophy and scaled down approximately to half the size of a prototype structure in geometry. It should be noted that the minimum scaling factor for test specimens is given as one-third in ACI's T1.1-01 *Acceptance Criteria for Moment Frames Based on Structural*

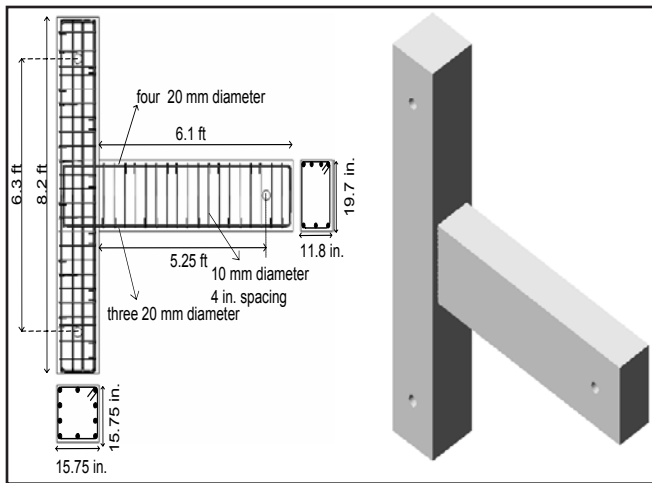


Fig. 1. Dimensions and reinforcement detail of monolithic specimen. Note: 1 in. = 25.4 mm; 1 ft = 0.3048 m.

Testing.²⁰ The cross section of the beams was 11.8 in. × 19.7 in. (300 mm × 500 mm), and the beam clear span was 5.25 ft (1600 mm). Hence, the shear span-to-beam depth ratio (a/h) was about 3.2. The reason for such a low a/h was to make the precast concrete connection govern the design at higher shear forces. The height of the column was 6.3 ft (1920 mm), and it had a square cross section with 15.75 in. (400 mm) dimensions. The cover thickness in the precast concrete beam and column was 0.8 in. (20 mm). **Figure 1** shows the dimensional detail of the subassembly.

Monolithic Specimen

The reference monolithic (M) specimen was designed according to the Turkish Civil Engineering Chamber code provisions for high seismic regions.²¹ For all specimens (monolithic and precast concrete), the column longitudinal reinforcement ratio was 2%, and spacing of the closed stirrups was approximately 4 in. (100 mm) at the beam-column joint core. As shown in Fig. 1, four and three $3/4$ -in.-diameter (20 mm) reinforcing bars were placed at the top and the bottom of the beam, respectively. The bottom reinforcement in the beam was less than the top reinforcement due to the gravity load effect.

For all specimens, except specimen GOK-W, the same grade $3/4$ -in.-diameter (20 mm) bars were used as longitudinal reinforcement and $3/8$ -in.-diameter (10 mm) reinforcing bars were used as lateral reinforcement. The yield and ultimate strength of the $3/4$ -in.-diameter (20 mm) reinforcing bars were 68.5 ksi (472 MPa) and 83.3 ksi (574 MPa), respectively, and the elongation at ultimate strength was 14%, measured on a gage length of 10 bar diameters. The compressive strength of the concrete for specimen M was 5800 psi (40 MPa).

Cast-in-Place in Column Connection

In the CIP in column (CIPC) connection detail, there was a gap at midheight of the precast concrete column (**Fig. 2**). The height of the gap was 19.7 in. (500 mm) and was

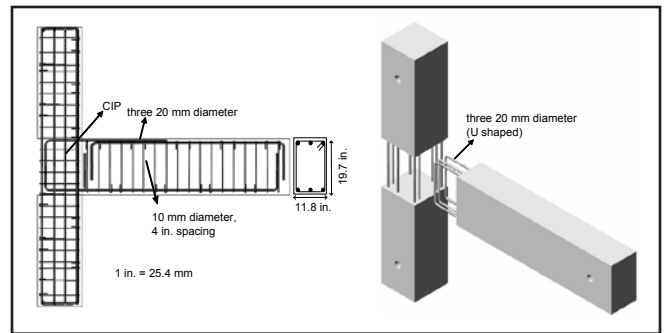


Fig. 2. Detail of cast-in-place in column connection. Note: 1 in. = 25.4 mm.

equal to the beam depth. In the precast concrete beam, three $3/4$ -in.-diameter (20 mm), U-shaped reinforcing bars were installed as flexural reinforcement at the connection region due to anchorage considerations. Additionally, there were three $3/4$ -in.-diameter (20 mm) reinforcing bars at the top and the bottom of the beam body as main reinforcement. In the assembly process, the precast concrete beam was seated through the gap on the precast concrete column. The concrete compressive strength for the precast concrete members was 7542 psi (52 MPa). In order to eliminate or delay the bond problem at the joint region where U-shaped reinforcing bars were used, concrete with 1.57 in. (40 mm) hooked steel fibers (volume fraction of fiber of 0.5%) was placed in the joint region. The compressive strength of the CIP concrete in the connection was 7687 psi (53 MPa). Due to the presence of U-shaped reinforcing bars, closed stirrups could not be installed; single leg ties were used in the column joint core instead.

Cast-in-Place in Beam Connection

A design concept similar to the CIPC specimen was also applied to the CIP in beam (CIPB) connection. The difference was the location of the connection region, which was 19.7 in. (500 mm) long and located at the joining end of the precast concrete beam (**Fig. 3**). Again, U-shaped reinforcing bars protruding from the column (four $3/4$ -in.-diameter [20 mm]) and from the beam (three $3/4$ -in.-diameter [20 mm]) for flexure were used in this region. Concrete compressive strength for the precast elements was 5800 psi (40 MPa). During the assembly process, reinforcing bars in the precast concrete beam were located between the bars protruding from the precast concrete column at an interlock-

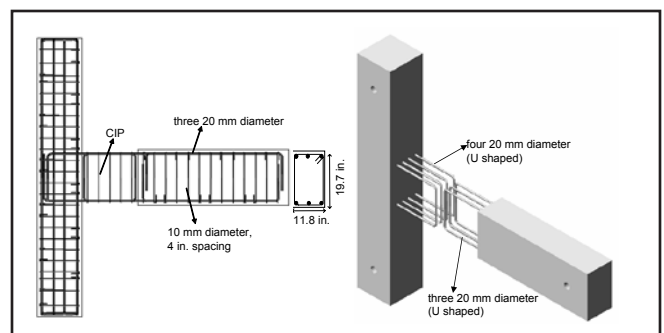


Fig. 3. Detail of cast-in-place in beam connection. Note: 1 in. = 25.4 mm.

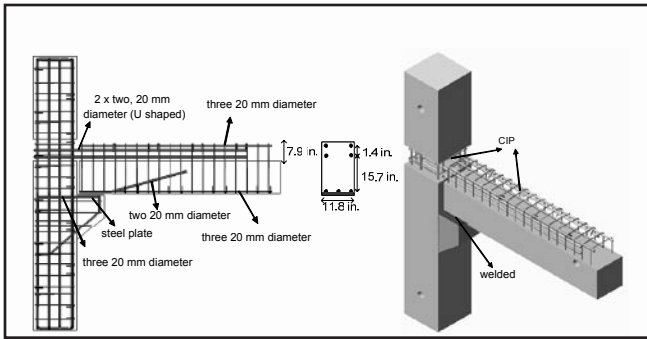


Fig. 4. Reinforcement detail and assembly process of composite connection. Note: 1 in. = 25.4 mm.

ing position. Steel fiber-reinforced concrete (with a 0.5% volume fraction and a compressive strength of 7107 psi [49 MPa]) was placed at the connection region. Single leg ties were used in the connection region.

Composite Connection

The composite (GOK-W) connection type ensured the continuity of the beam's bottom reinforcement by welding and the top reinforcement by placing cast-in-place concrete through the gap in the column. GOK-W is a common connection used by Turkish precast concrete producers. This test specimen was designed and produced by GOK Construction Co. The cross-sectional dimension of the square precast concrete beam was 11.8 in. (300 mm). The CIP section of the subassembly consisted of a region with a depth of 7.9 in. (200 mm) along the precast concrete beam and the gap in the middle of the column (**Fig. 4**). Three $\frac{3}{4}$ -in.-diameter (20 mm) reinforcing bars acted as the main reinforcement at the bottom of the beam, and they were welded to a steel plate with dimensions of 11.8 in. \times 9.8 in. \times 0.6 in. (300 mm \times 250 mm \times 15 mm). Additionally, two $\frac{3}{4}$ -in.-diameter (20 mm) reinforcing bars bent up at 20 degrees to the horizontal were welded to the same plate to secure the anchorage of the steel plate to the precast concrete beam (**Fig. 4**). This detailing also created additional positive flexural moment capacity. Moreover, two rows of $\frac{3}{4}$ -in.-diameter (20 mm) U-shaped flexural bars were installed through the gap in the column as top reinforcement for the beam during the assembly process. The center-to-center distance between these two rows was 1.4 in. (36 mm). Main reinforcing bars for the precast concrete corbel were welded to a steel plate, which was later welded to the bottom plate of the beam for continuity. Cast-in-place concrete was placed in the upper part of the beam and in the gap of the column. All $\frac{3}{4}$ -in.-diameter (20 mm) reinforcing bars were weldable steel with a yield and ultimate strength of 73 ksi (503 MPa) and 96 ksi (662 MPa), respectively. The elongation of the $\frac{3}{4}$ -in.-diameter (20 mm) reinforcing bars at ultimate strength was 13%, measured on a gage length of 10 bar diameters. The compressive strength of the precast concrete elements was 8267 psi (57 MPa), and the compressive strength of the CIP concrete was 7977 psi (55 MPa) for specimen GOK-W.

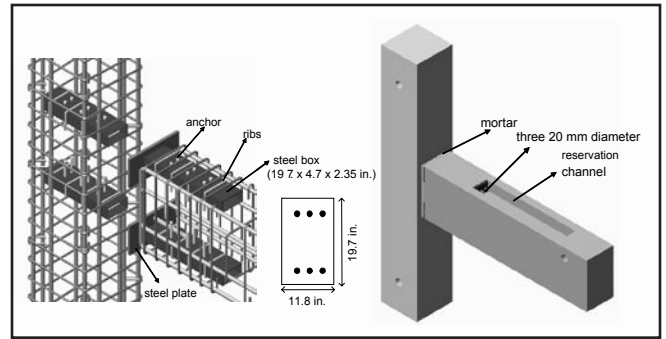


Fig. 5. Connection detail and overall view of modified bolted connection. Note: 1 in. = 25.4 mm.

Bolted Connection

The aim of the bolted connection types was to minimize the field work during the assembly process. In the proposed bolted connection detail, rectangular steel boxes were used instead of steel pipes for through holes (**Fig. 5**). Steel boxes allowed more dimensional tolerance to compensate for production errors and more space for multiple bolts. This connection type is more suitable for low level of gravity load-induced shear forces, where precast concrete members, such as double tees and hollow-core slabs, were oriented parallel to the beam axis.

Figure 5 shows the reinforcement detail and the overall view of the precast concrete members for the bolted (Mod-B) connection type. The precast concrete beam has a channel at the top and bottom of the cross section to allow for installation of the bolts during the assembly process. The length of the channel was 39.4 in. (1000 mm) with cross-sectional dimensions of 5.9 in. \times 3.9 in. (150 mm \times 100 mm). Rectangular steel boxes, 19.7 in. (500 mm) long with cross-sectional dimensions of 4.7 in. \times 2.35 in. (120 mm \times 60 mm), were located at the joining end of the beam and through the column along the same axis. In this region of the beam, closed stirrups were installed with 2.8 in. (70 mm) spacing. Moreover, steel plates were placed at the top and bottom of the beam cross section to delay crushing of the beam concrete adjacent to the column face. These steel plates were also connected to each other by two $\frac{3}{8}$ -in.-diameter (10 mm) bars welded to either plate.

The precast members were produced with a 4060 psi (28 MPa) design compressive strength concrete. During the assembly process, the 0.6 in. (15 mm) gap between the precast concrete beam and the column was filled with a self-leveling, nonshrink grout. The compressive strength of the grout was 8412 psi (58 MPa). After 24 hours, three $\frac{3}{4}$ -in.-diameter (20 mm) reinforcing bars (with machine-threaded ends) were placed into the steel boxes located at the top and the bottom of the connection. Then an initial pretensioning force of 25.8 lb-ft (35 N-m) of torque was applied with a torque wrench. Later, the torque was increased to 88.5 lb-ft (120 N-m), resulting in a 203 psi (1.4 MPa) clamping stress at the beam-column interface; the stress developed in the reinforcing bars was 16 ksi (110 MPa). The bolts were about 2.75 in. (70 mm) from top and bottom fiber of the beam. Fi-

nally, the steel boxes were filled with the same grout.

In the first test of this bolted connection, the steel boxes were welded directly to the precast concrete beam's shear reinforcement and this type of connection was called bolted (B). During the test, sliding of the steel boxes with respect to the beam concrete was observed. To solve this problem, steel bars were welded around the steel boxes to serve as ribs. In addition, rods passing through the box cross section were added to eliminate any possible sliding of the infill grout with respect to the steel box itself. The connection type after these modifications was called modified bolted (Mod-B). In this detail, the compressive strength of concrete in the precast members was 4350 psi (30 MPa) and the compressive strength of the grout was 5220 psi (36 MPa).

TESTING PROCEDURE

The test setup was designed to apply the procedure and scheme specified in ACI's T1.1-01: *Acceptance Criteria for Moment Frames Based on Structural Testing*.²⁰ Figure 6 presents the test setup and the locations of the deformation measurements. The precast concrete column was supported on a pinned connection at its base, and the top of the column was free to move and rotate. A roller-supported "free end" was designed for the beam; hence, the points of contra flexure for both the beam and the column were achieved within the test setup. An axial load of approximately 10% of the column compressive capacity was applied to the columns in all specimens with a closed frame and a hydraulic ram mounted on top of the column (Fig. 6). The lateral load applied was gradually increased to achieve the predetermined story drifts. Several linear variable displacement transducers (LVDTs) were mounted on the test specimens to measure the net story drift, joint rotation, gap openings, and shear deformations. The net column top displacement (Δ_{cnet}) was calculated by subtracting the column base lateral displacement and the vertical beam tip displacement from the lateral displacement measurement at the column top. Top displacement of the column (Δ_{ct}) was measured by using two 7.9-in.-capacity (200 mm) LVDTs mounted at the level of the hydraulic actuator. Column base displacement (Δ_{cb}) was measured at the

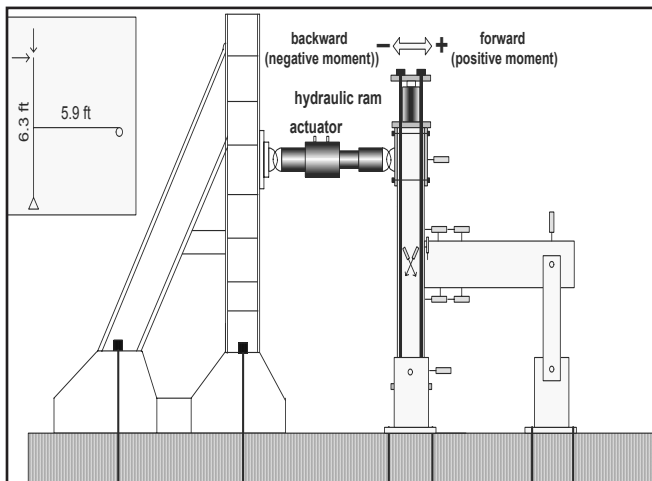


Fig. 6. Test setup and instrumentation. Note: 1 ft = 0.3048 m.

pin support level. At this level, lateral displacement readings should be zero in the ideal test rig. Also, the vertical displacement (Δ_{bv}) of the beam tip should be zero. Therefore, these displacement readings were monitored continuously and the net column top displacement, which will yield the level of story drift, was calculated according to Eq. (1). A 6.3/5.9 ratio is used because of the geometric compatibility.

$$\Delta_{cnet} = \Delta_{ct} - \Delta_{cb} - \left(\frac{6.3}{5.9} \times \Delta_{bv} \right) \quad (1)$$

Figure 7 shows the loading protocol that was taken from ACI's T1.1-01: *Acceptance Criteria for Moment Frames Based on Structural Testing*.²⁰ The first cycles (0.15% and 0.20%) were in the elastic range. Three fully reversed cycles were applied at each drift level. All data were collected with a 50 Hz data acquisition box. Cracks, gap openings, and failures were monitored in successive three-cycle intervals. All test specimens were loaded ultimately until the 4% interstory drift ratio. The test was terminated before the 4% drift level only in cases of a premature failure of the connection, mainly due to the rupture of flexural reinforcing bars.

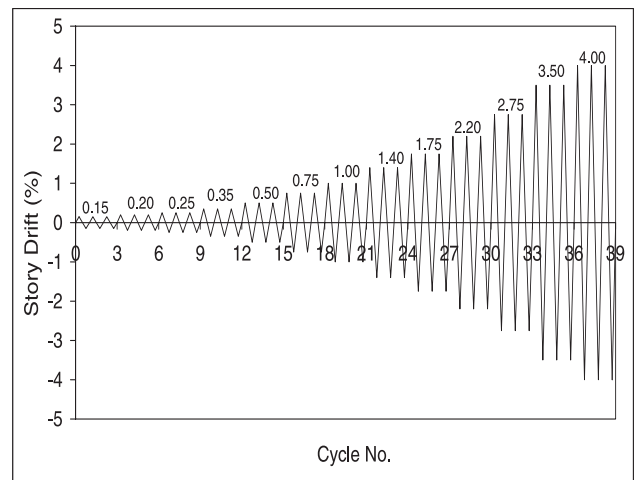


Fig. 7. Loading history of cycles.



Fig. 8. Damage in monolithic specimen at 4% drift level.

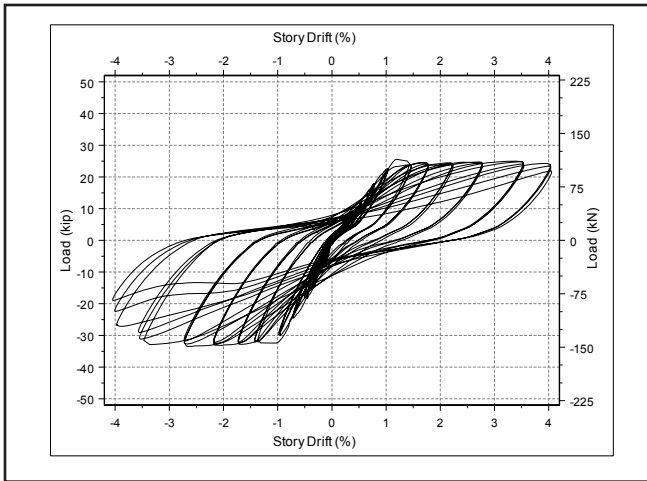


Fig. 9. Lateral load versus story drift response of monolithic specimen.

TEST RESULTS

Monolithic Specimen

The response of specimen M was nearly elastic during the first two successive cycles. At the 0.25% story drift level, minor flexural cracks were observed on the beam at a distance of 10 in. (250 mm) from the column face. At the 0.75% story drift level, the first hairline diagonal crack was observed at the beam-column joint core. The first diagonal cracking in the beam was observed at the 1.4% story drift level. Spalling of concrete at the end of the beam joining the column started at the 3.5% drift level, and the beam bottom flexural reinforcement buckled at the 4% story drift level (**Fig. 8**). Cracks were well distributed over the beam end region. **Figure 9** presents the lateral load versus story drift response of specimen M. Behavior of specimen M was good in terms of ductility and energy dissipation. No evident pinching effect was observed on the reversed cyclic response, and there was no significant strength degradation until the 4% story drift level. The ultimate lateral load capacities of the specimen for forward and backward cycles were 25.6 k (114 kN) and -33.5 k (-149 kN), respectively.

Cast-in-Place in Column Connection

The first flexural crack in specimen CIPC was observed at the 0.25% story drift level at the beam column interface. No diagonal cracking was observed at the joint core throughout the test because of the steel fiber-reinforced concrete. Most of the cracks were concentrated on the beam at the column face. **Figure 10** shows the response of specimen CIPC. It is observed that there is a shift in the drift amplitudes (**Fig. 10**) with respect to the predetermined loading history (**Fig. 7**), and this shift may be explained by the excessive settlement that occurred at the column supports due to a defective testing rig design. This problem was eliminated for the rest of the test specimens. The behavior of specimen CIPC was similar to that of specimen M, up to the 2.75% story drift level. The yielding load level in both specimens was reached around the 1.0% drift level. After that level, the strength degradation was more pronounced in the CIPC specimen than in

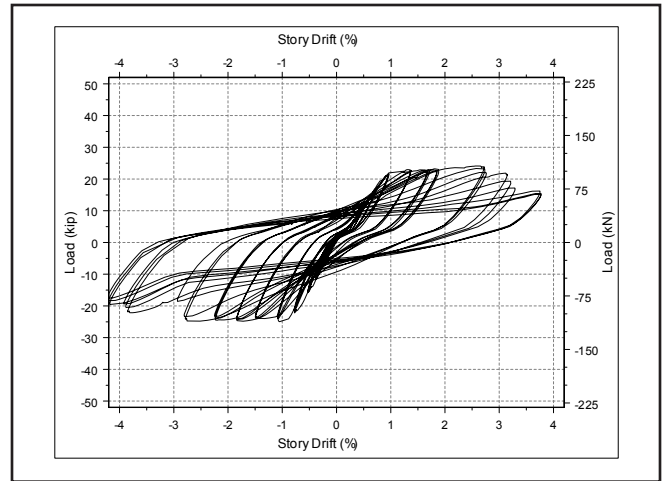


Fig. 10. Lateral load versus story drift response of specimen cast-in-place in column connection.

specimen M. The reasons for the rapid degradation were the crushing of concrete at the top and bottom of the beam cross section and buckling of the reinforcement (**Fig. 11**). The reduction in the beam cross section due to spalling of concrete resulted in sliding of the precast beam relative to the precast column. This type of response was first observed at the 2.2% story drift level and rapidly increased to 0.6 in. (15 mm) at the 3.5% drift level. No bond problem was observed throughout the test. The maximum lateral loads attained were 24.1 k (107 kN) in forward and -25.0 k (-111 kN) in backward cycles. Plastic hinging took place in the beam near the column face.

Cast-in-Place in Beam Connection

The first visible cracks were observed along the CIP concrete and the precast concrete element interface both in the beam and the column at the 0.25% story drift level. Generally, the flexural cracks were concentrated at these interfaces. A hairline diagonal crack at the beam-column joint core was first observed at 1.75% story drift. When the story drift level reached 2.75%, the gap opening width between the column face and the CIP interface reached approximately 0.3 in. (8 mm). The crack concentration then relocated to the beam-



Fig. 11. Damage in specimen cast-in-place in column connection at 4% drift level.

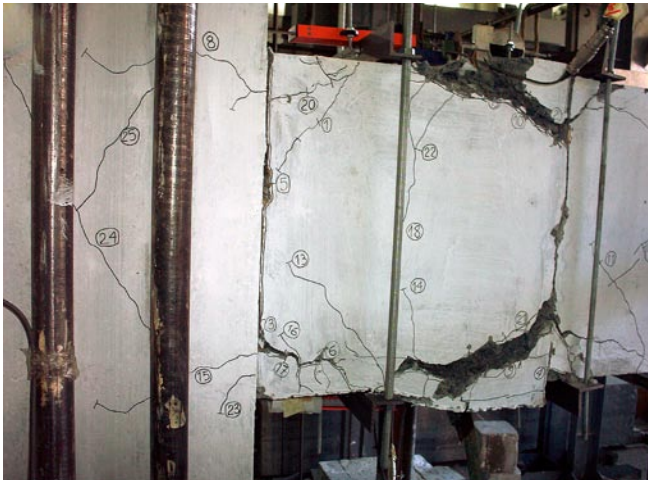


Fig. 12. Damage in specimen cast-in-place in beam connection at 4% drift level.

CIP interface, and widening of this crack accelerated at higher drift levels, eventually leading to the failure of specimen (Fig. 12). The CIP concrete experienced minimal cracking and behaved nearly linear throughout the successive load cycles. Figure 13 shows the response of specimen CIPB, which was very similar to specimen M. No pinching effect or sliding of the CIP concrete over the column was observed throughout the reversed cyclic response of specimen CIPB. The recorded maximum lateral load was 31.8 k (142 kN) and -33.9 k (-151 kN) for forward and backward cycles, respectively.

Composite Connection

During the assembly process, the embedded steel plates of the corbel and beam were welded together to secure the continuity of the beam bottom reinforcement. It was observed that the bond of approaching reinforcing bars in the vicinity of the weld location was damaged, resulting in hairline cracks in the concrete parallel to the bar axes. The first flexural crack in the beam was observed at the 0.5% story drift level and was located 10 in. (250 mm) away from the precast concrete column. This distance corresponds to the tip of the precast concrete corbel. Flexural cracks on the beam were distributed



Fig. 14. Damage in composite connection specimen at 3.5% drift level.

evenly. At the 1.4% story drift level, a diagonal crack was observed at the corbel-column region. Diagonal cracking at the beam-column joint core was first observed at 2.2% story drift. The failure of specimen GOK-W occurred suddenly with the rupture of the beam's bottom reinforcement at the 3.5% story drift level (Fig. 14). Figure 15 shows the lateral load versus story drift response of the GOK-W subassembly. The ductility of specimen GOK-W was less than that of previous test specimens. The early rupture of the reinforcement may well be explained with the changing mechanical properties of the steel due to the welding done during the preparation of steel cages prior to molding. The ultimate loads were 50.9 k (226 kN) for forward and -47.1 k (-209 kN) for backward cycles.

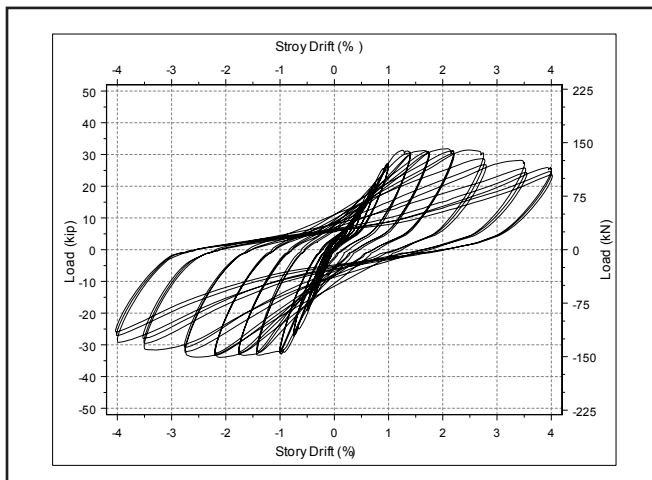


Fig. 13. Lateral load versus story drift response of specimen cast-in-place in beam connection.

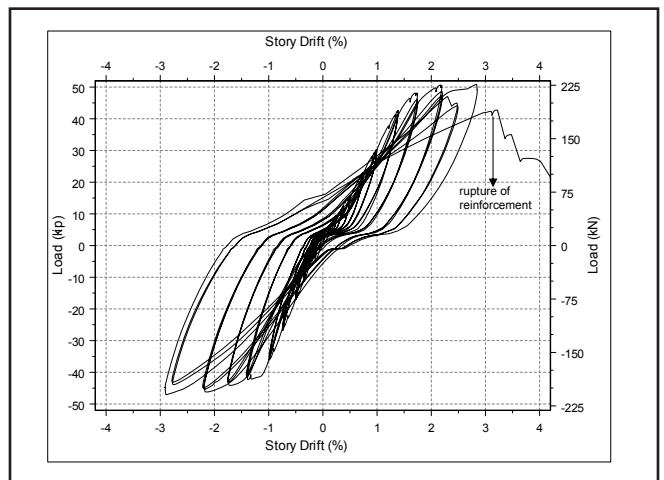


Fig. 15. Lateral load versus story drift response of composite connection specimen.

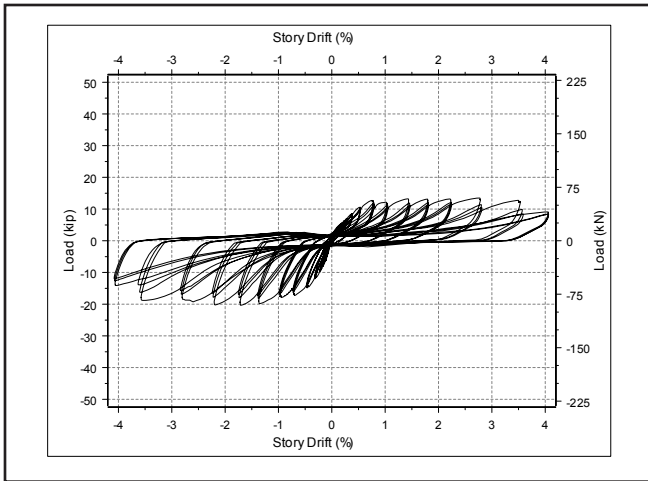


Fig. 16. Lateral load versus story drift response of bolted specimen.

Bolted Connection

The cyclic response of specimen B was unsatisfactory, as shown in **Fig. 16**. Although the flexural cracks at the beam-column interface were first observed at the 0.5% story drift level, the sliding of steel box relative to the precast concrete beam was accelerated beyond this level (**Fig. 17**). Therefore, the bolts could not reach their yielding load level. The deficiencies of specimen B were highlighted during and after the test. Hence, specimen Mod-B was designed and constructed. During the test of specimen Mod-B, no relative slip between the steel boxes and the beam concrete was observed. Flexural cracks were concentrated at the beam-column interface, and there was no diagonal crack observed at the joint core. Steel plates at the face of the beam (**Fig. 5**) prevented the crushing of concrete at lower drift levels. At the 3.5% story drift level, top bolts were ruptured and the experiment was terminated. The behavior of specimen Mod-B may well be considered satisfactory. **Figures 18** and **19** present the response of the specimen Mod-B and the damage accumulation, respectively. The overall performance of the specimen Mod-B was better than that of specimen M and other types of connections. Due to the pretensioning applied



Fig. 17. Damage in bolted specimen at 4% drift level.

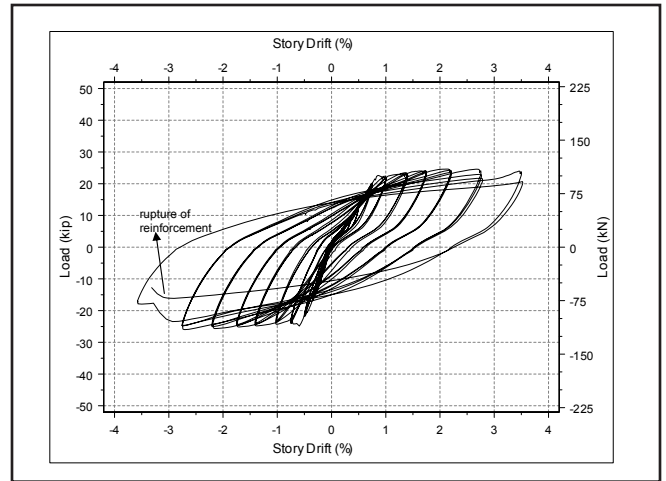


Fig. 18. Lateral load versus story drift response of modified bolted connection specimen.

to the bolts, initial stiffness was greater in specimen Mod-B and the bolts yielded at smaller drift levels compared with the other subassemblies. Specimen Mod-B behaved similarly to a friction damper with a fuller hysteresis curve free from pinching. On the other hand, at higher story drift levels, sliding was observed between the precast concrete beam and column. The maximum recorded lateral loads were 24.6 k (110 kN) and -26.0 k (-116 kN) during the last forward and backward cycles, respectively.

Evaluation of Test Results

The M, CIPC, CIPB, GOK-W, and Mod-B test specimens were compared according to their strength predictions, stiffness degradation properties, and energy dissipation properties. All specimens were compared with non-dimensional values to eliminate different connection strengths. Discussion of specimen B is omitted because of its poor performance and the existence of its redesigned companion, specimen Mod-B.

Strength—Prior to testing, yield (M_y) and ultimate (M_u)

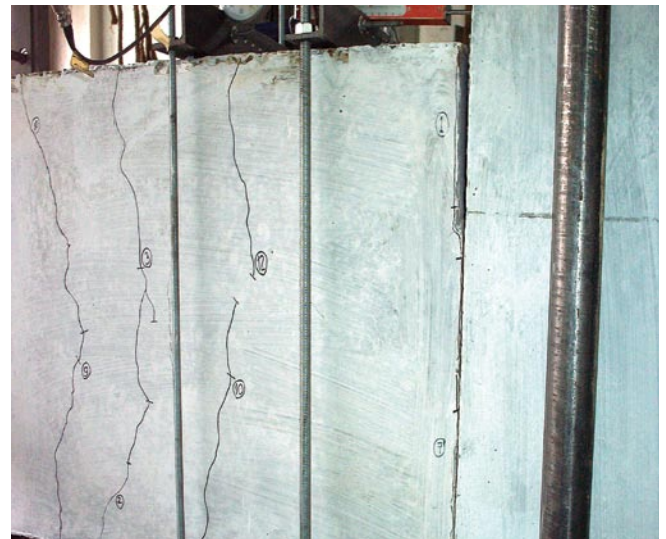


Fig. 19. Damage in modified bolted connection specimen at 3.5% drift level.

moment capacities of each connection were calculated for the positive (M_y^+ , M_u^+) and negative (M_y^- , M_u^-) cycles through conventional hand modeling with a rectangular concrete stress block and yield and ultimate strength of the reinforcing bars. **Table 1** gives the experiment results and predicted capacities. The predictions are very important to define the connection performance in terms of flexural strength. All connections reached their calculated yield and ultimate moment capacities. At high drift levels, the beam's bottom concrete cover spalled off and its bottom flexural reinforcement buckled. Therefore, the ratios of ultimate moment capacities to the predicted values for forward cycles were smaller than those for backward cycles (negative moment). The capacity prediction for the backward cycle of specimen GOK-W was less than the experimentally measured value due to the existence of the corbel, which served as a haunched beam end. In addition, the test load capacities of specimen Mod-B were greater than the predicted values. This may be due to the existence of steel plates located at the surface of the beam and the confining effect of closed stirrups located in the beam at the connection region.

Stiffness Degradation—The secant stiffness (K_{sec}) calculated at the last cycle of each successive story drift level was used for comparison of stiffness degradation among test specimens. The secant stiffness is defined as the slope of the straight line between the maximum drift levels of that specific load cycle. It is also called peak-to-peak stiffness and is illustrated in **Fig. 20**. Each secant stiffness value of a specific specimen was normalized (K_{norm}) with respect to the secant stiffness measured at the 0.15% story drift level for a possible comparison between the Phase I specimens. The use of normalized secant stiffness allows easy comparison with other test specimens and avoids subjective assumptions. The stiffness values for specimen GOK-W were computed up to the 2.75% story drift level because it failed during the 3.5% load cycle. Besides, the stiffness of specimen Mod-B was calculated for the first cycle of 3.5% story drift because the con-

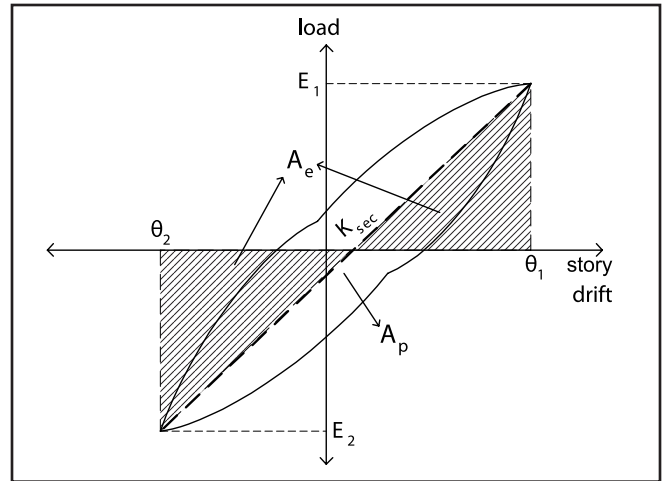


Fig. 20. Representation of secant stiffness and equivalent damping ratio.

nection failed during the second cycle of this load step.

It is observed that the stiffness degradation of specimens M, CIPC, and CIPB are very similar, especially at higher drift levels. The loss of initial stiffness for these three connections was approximately 75% to 80% at the end of the last cycle (**Fig. 21**). On the other hand, there was no significant stiffness degradation in specimen GOK-W up to the 1.0% story drift level. At 2.75% story drift, approximately 50% of the initial stiffness was reserved in specimen GOK-W. The initial stiffness of specimen Mod-B was greater than that of the other specimens; however, stiffness degradation was more pronounced due to the gap opening at the column surface.

Energy Dissipation—To discuss the energy dissipation characteristics of the test specimens, the equivalent viscous damping ratio (ζ_{eq}) was plotted against the story drift (**Fig. 22**). Energy dissipation of a test specimen was computed from the last cycle of each successive story drift level. Chopra defined the equivalent viscous damping ratio as the energy dissipated in a vibration cycle of the actual structure

Table 1. Comparison of Test Results and Capacity Predictions

Specimen	Experimental (k-in.)*				Calculated (k-in.)*				Ratio			
	(1)	(2)	(3)	(4)	(5)	(6)	(7)	(8)	(9)	(10)	(11)	(12)
	M_y^+	M_y^-	M_u^+	M_u^-	M_y^+	M_y^-	M_u^+	M_u^-	(1)/(5)	(2)/(6)	(3)/(7)	(4)/(8)
M	1692	2248	1942	2537	1664	2230	1956	2469	1.02	1.01	0.99	1.03
CIPC	1652	1825	1827	1891	1673	1673	1956	1956	0.99	1.09	0.93	0.97
CIPB	1727	1792	1792	1927	1664	1664	1956	1956	1.04	1.08	0.92	0.99
GOK-W	3076	3118	3253	3568	3000	2319	3354	2903	1.03	1.35	0.97	1.23
Mod-B	1629	1707	1864	1966	1531	1531	1682	1682	1.06	1.11	1.11	1.17

Note: M = monolithic specimen; CIPC = cast-in-place column connection; CIPB = cast-in-place beam connection; GOK-W = composite connection; Mod-B = modified bolted connection. 1 k-in. = 0.113 kN-m.

* M_y^+ and M_u^+ are yield and ultimate moment capacities, respectively; M_y^+ and M_u^+ , and M_y^- and M_u^- are the positive and negative cycles, respectively.

CONCLUSIONS

Based on the test results, assembly process of connection, and observations made during thereversed cyclic test, the following conclusions are drawn:

- Specimen Mod-B showed the best performance in terms of strength, ductility, and energy dissipation in addition to ease and speed of construction.
- All tested precast concrete connections, except specimen B, are suitable for high seismic zones in terms of strength properties and energy dissipation.
- The hysteresis behaviors of specimens CIPC, CIPB, and Mod-B are similar to those of specimen M. Specimen GOK-W with welding yielded an inferior performance compared with the other types of connections.
- The precast concrete connections, except specimen B, reached their calculated yield and ultimate flexural moment capacities.
- Except for specimen GOK-W, all specimens could sustain up to 3.5% story drift. This means they have enough ductility for seismic loads. Excessive welding may adversely affect the mechanical properties of the reinforcement and is believed to be the cause of the inferior performance of specimen GOK-W.
- Equivalent damping ratios of the precast concrete connections are similar or better than the monolithic system.
- Pinching effect and excessive bond deterioration were not observed in the CIP connections due to the use of steel fiber concrete and U-shaped reinforcing bars.
- For bolted connections, there is a risk of sliding of the steel box or pipe with respect to the beam concrete. Therefore, designers should consider detailing steel boxes or pipes to avoid the sliding problem by welding ribs to the surface of the steel boxes or pipes.
- During assembly, CIP connections need extra formwork on-site and also increase time and cost. In addition, high quality-control procedures are needed for welded connection. On the other hand, assembly of bolted connections is relatively quick.

ACKNOWLEDGMENTS

The research project was funded by the Scientific and Technical Research Council of Turkey (TUBITAK) (Project No: ICTAG I589) and the Turkish Precast Concrete Association. The authors gratefully acknowledge AFAPREFABRIK, GOK Construction, SIKKA, BEKSA, and AKCANSANSA companies for their invaluable guidance and support. Special thanks go to Bogazici University's Structures Laboratory technical staff. The authors also express their appreciation to the *PCI Journal* reviewers for their valuable suggestions and constructive comments.

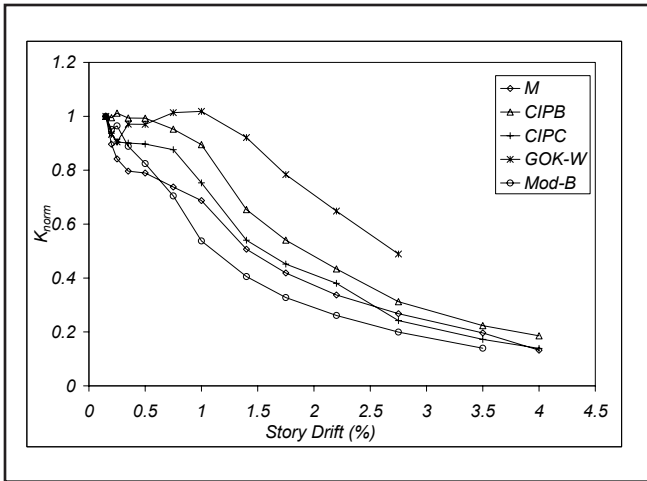


Fig. 21. Stiffness degradation of specimens.

to an equivalent viscous system.²² For an actual structure, the resisting force–displacement relation obtained from an experiment under cyclic loading is illustrated in Fig. 20. The energy dissipated in the actual structure is given by the area A_p enclosed by the hysteresis loop. Area A_e is the strain energy that is calculated from the assumed linear elastic behavior of the same specimen. This definition is formulated in Eq. (2).¹⁹

$$\zeta_{eq}(\%) = \frac{1}{2} \frac{A_p}{A_e} \times 100 \quad (2)$$

In general, equivalent viscous damping increased with increasing story drift (Fig. 22). The trends of specimens M, CIPC, CIPB, and GOK-W were very similar. The response of the Mod-B connection in terms of energy dissipation was more satisfactory than that of the monolithic specimen M. At 2% story drift, which may be called the design drift level, the equivalent viscous damping ratio of specimen Mod-B was about 20% to 25%, while the other connections were experiencing 10% to 15% damping. Also, the damping ratio of specimen Mod-B reached 35% at the 3.5% story drift level.

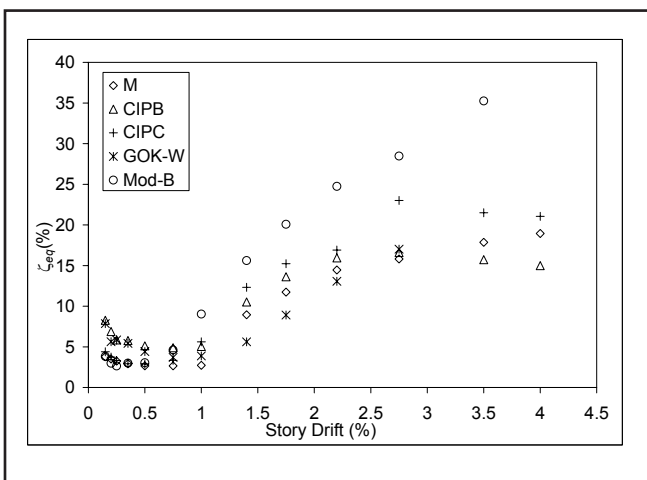


Fig. 22. Equivalent viscous damping ratios versus story drift response.

REFERENCES

1. Restrepo, J. I., R. Park, and A. H. Buchanan. 1995. Tests on Connections of Earthquake Resisting Precast Reinforced Concrete Perimeter Frames of Buildings. *PCI Journal*, V. 40, No. 4 (July–August): pp. 44–61.
2. Alcocer, S. M., R. Carranza, D. Perez-Navaratte, and R. Martinez. 2002. Seismic Tests of Beam to Column Connections in a Precast Concrete Frame. *PCI Journal*, V. 47, No. 3 (May–June): pp. 70–89.
3. Rodriguez, M. E., and J. J. Blandon. 2005. Tests on Half-Scale Two-Story Seismic-Resisting Precast Concrete Building. *PCI Journal*, V. 50, No. 1 (January–February): pp. 94–114.
4. Blandon, J. J., and M. E. Rodriguez. 2005. Behavior of Connections and Floor Diaphragms in Seismic-Resisting Precast Concrete Buildings. *PCI Journal*, V. 50, No. 2 (March–April): pp. 56–75.
5. Soubra, K. S., J. K. Wight, and A. E. Naaman. 1993. Cyclic Response of Fibrous Cast-in-Place Connections in Precast Beam-Column Subassemblages. *ACI Structural Journal*, V. 90, No. 3 (May–June): pp. 316–323.
6. Vasconez, R.M., A. E. Naaman, and J. K. Wight. 1998. Behavior of HPFRC Connections for Precast Concrete Frames Under Reversed Cyclic Loading. *PCI Journal*, V. 43, No. 6 (November–December): pp. 58–71.
7. Bhatt, P., and D. W. Kirk. 1985. Test on an Improved Beam Column Connection for Precast Concrete. *ACI Journal*, V. 82, No. 6 (November–December): pp. 834–843.
8. Seckin, M., and H. C. Fu. 1990. Beam-Column Connections in Precast Reinforced Concrete Construction. *ACI Structural Journal*, V. 87, No. 3 (May–June): pp. 252–261.
9. Ochs, J. E., and M. R. Ehsani. 1993. Moment Resistant Connections in Precast Concrete Frames for Seismic Regions. *PCI Journal*, V. 38, No. 5 (September–October): pp. 64–75.
10. Stanton, J. F., N. M. Hawkins, and T. R. Hicks. 1991. PRESSS Project 1.3: Connection Classification and Evaluation. *PCI Journal*, V. 36, No. 5 (September–October): pp. 62–71.
11. Yee, A.A. 1991. Design Considerations for Precast Prestressed Concrete Building Structures in Seismic Areas. *PCI Journal*, V. 36, No. 3 (May–June): pp. 40–55.
12. Mast, R. F. 1992. A Precast Concrete Frame System for Seismic Zone Four. *PCI Journal*, V. 37, No. 1 (January–February): pp. 50–64.
13. French, C. W., O. Amu, and C. Tarzikhan. 1989. Connections between Precast Elements—Failure Outside Connection Region. *Journal of Structural Engineering*, V. 115, No. 2: pp. 316–340.
14. French, C. W., M. Hafner, and V. Jayashankar. 1989. Connection between Precast Elements—Failure within Connection Region. *Journal of Structural Engineering*, V. 115, No. 12: pp. 3171–3192.
15. Priestley, M. J. N. 1996. The PRESSS Program—Current Status and Proposed Plans for Phase III. *PCI Journal*, V. 41, No. 2 (March–April): pp. 22–40.
16. Ghosh, S. K., S. D. Nakaki, and K. Krishan. 1997. Precast Structures in Region of High Seismicity: 1997 UBC Design Provision. *PCI Journal*, V. 42, No. 6 (November–December): pp. 76–93.
17. International Conferences of Building Officials (ICBO). 1997. *Uniform Building Code: V. 2, Structural Engineering Design Provisions*. Whittier, CA: ICBO.
18. Hawkins, N. M., and S. K. Ghosh. 2000. Proposed Revisions to 1997 NEHRP Recommended Provisions for Seismic Regulations for Precast Concrete Structures Part 2—Seismic-Force-Resisting Systems. *PCI Journal*, V. 45, No. 5 (September–October): pp. 34–44.
19. Nakaki, S.D., R. E. Englekirk, and J. L. Plaehn. 1994. Ductile Connectors for a Precast Concrete Frame. *PCI Journal*, V. 39, No. 5 (September–October): pp. 46–59.
20. American Concrete Institute (ACI) Innovation Task Group 1 and Collaborators and ACI Committee 374. 2001. T1.1-01/T1.1R-01: Acceptance Criteria for Moment Frames Based on Structural Testing. Farmington Hills, MI: ACI.
21. Turkish Civil Engineering Chamber. 1998. *Specifications for Structures to be Built in Disaster Areas*. Turkey: Turkish Civil Engineering Chamber.
22. Chopra, A. K. 1995. *Dynamic of Structures—Theory and Applications to Earthquake Engineering*. International Edition. New Jersey: Prentice Hall.

APPENDIX: NOTATION

a/h	= shear span-to-beam depth ratio
A_e	= strain energy stored in the subassembly through linear elastic behavior
A_p	= energy dissipated by the subassembly; enclosed by the hysteresis loop
K_{norm}	= normalized secant stiffness of the subassembly
K_{sec}	= secant stiffness of the subassembly
M_u	= ultimate moment capacity of the connection
M_y	= yield moment capacity of the connection
Δ_{bv}	= beam tip vertical displacement
Δ_{cb}	= column base displacement
Δ_{cnet}	= column top net displacement
Δ_{ct}	= column top displacement
ζ_{eq}	= equivalent viscous damping ratio

PCI Journal - Issue Archives

[Home](#)

[Home](#) > [Publications](#) > [PCI Journal](#)



This is a back issue of journal. Use the links below file of the story you wish to see. If you do not have Reader you can download one [here](#).

May-June 2006 TOC

<< Next Issue [may-jun](#) 2006 Previous Issue >>

Inspired Design and International Partners Deliver Architectural Art and U Salt Lake City

Moshe Safdie, Isaac Franco, Steve Crane, Alejandro Fastag K., Don. C. Hokanson
 JL-06-MAY-JUNE-1.PDF - 699.4 KB PDF FILE

Fundamentals of Launching a Precast Concrete Segmental Operation for E Projects

Arthur M. Palmer
 JL-06-MAY-JUNE-2.PDF - 1.7 MB PDF FILE

Codification of Precast Seismic Structural Systems: An Update

S.K. Ghosh and Neil M. Hawkins
 JL-06-MAY-JUNE-3.PDF - 166.1 KB PDF FILE

General Solution of Flexural Strength of Bonded Prestressed Concrete Sec

Domingo J. Carreira
 JL-06-MAY-JUNE-4.PDF - 1.6 MB PDF FILE

Ductile Connections in Precast Concrete Moment Resisting Frames

Onur Ertas, Sevket Ozden, and Turan Ozturan
 JL-06-MAY-JUNE-5.PDF - 1.3 MB PDF FILE

Cherrydale Elementary School, Greenville, South Carolina

George Nasser
 JL-06-MAY-JUNE-6.PDF - 1.5 MB PDF FILE

Grant Park Tower, Minneapolis, Minnesota

George Nasser
 JL-06-MAY-JUNE-7.PDF - 1.5 MB PDF FILE

Industry News

Industry News

JL-06-MAY-JUNE-8.PDF - 2.5 MB PDF FILE

Reference Cards

Reference Cards

JL-06-MAY-JUNE-9.PDF - 165.9 KB PDF FILE

Chairman's Message

Robert McCormack

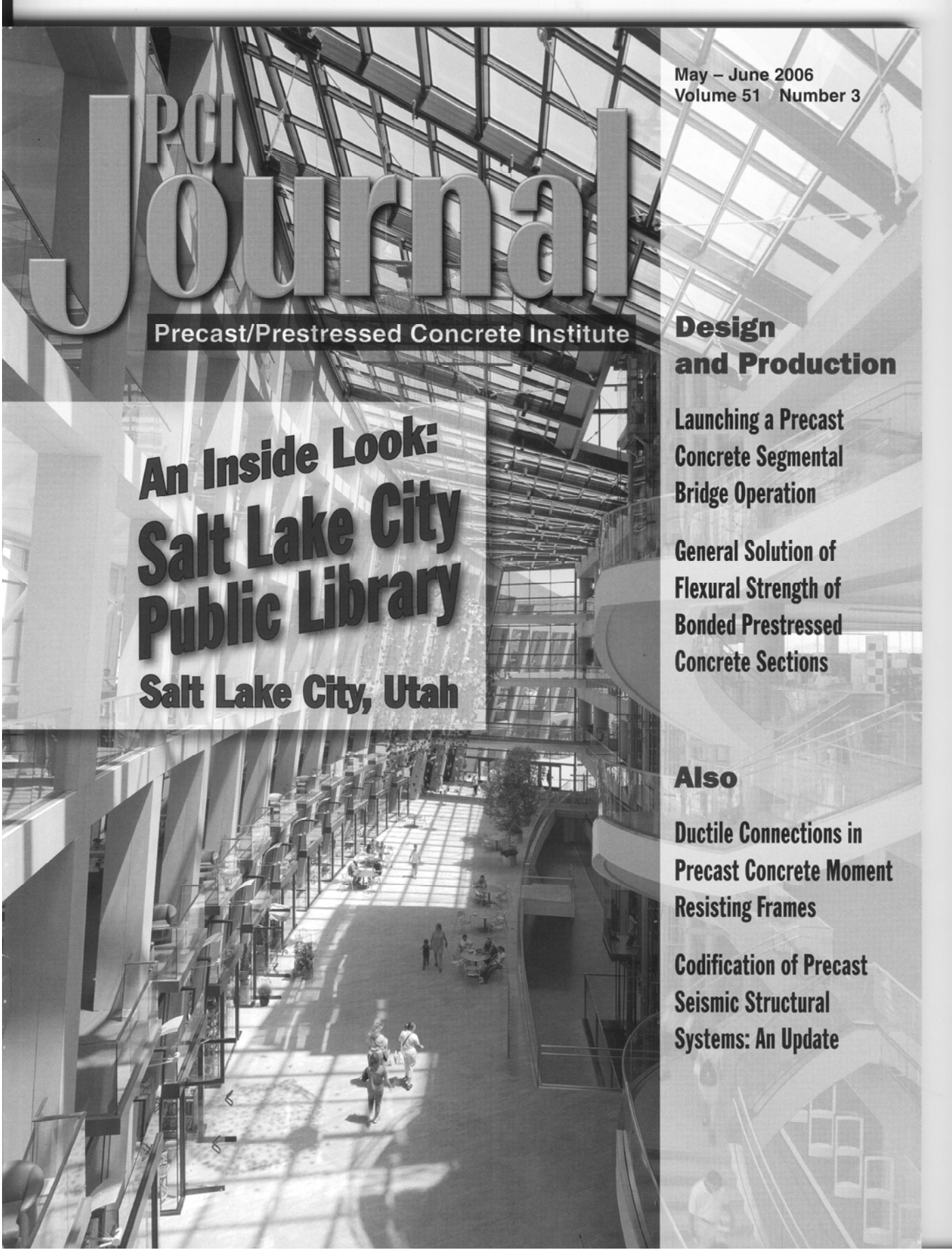
JL-06-MAY-JUNE-10.PDF - 84.2 KB PDF FILE

Technical Publications

Review of Technical Publications

JL-06-MAY-JUNE-11.PDF - 105.8 KB PDF FILE

Hosted by [InterActive Twist](#) a division of Leader Graphic Design, Inc.



May – June 2006
Volume 51 Number 3

JPCI Journal

Precast/Prestressed Concrete Institute

**An Inside Look:
Salt Lake City
Public Library
Salt Lake City, Utah**

Design and Production

**Launching a Precast
Concrete Segmental
Bridge Operation**

**General Solution of
Flexural Strength of
Bonded Prestressed
Concrete Sections**

Also

**Ductile Connections in
Precast Concrete Moment
Resisting Frames**

**Codification of Precast
Seismic Structural
Systems: An Update**

PCI Journal

EDITORIAL

Emily Lorenz, P.E.
Editor-in-Chief
(elorenz@pci.org)

Michelle Burgess
Associate Editor
(mburgess@pci.org)

Susan C. McCraven
Engineering Editor
(suemccraven@ameritech.net)

Ann Lopez
Administrative Assistant, *PCI Journal*
(alopez@pci.org)

George D. Nasser
Editor Emeritus

PRODUCTION

Jennifer Lee Atkin
Manager, Production
(jatin@pci.org)

Ed Derwent
Associate, Graphic Design
(ederwent@pci.org)

Paul Grigonis
Associate, Graphic Design
(pgrigonis@pci.org)

Keith Ulrich
Manuscript Editor
(kulrich@pci.org)

ADVERTISING SALES

Chuck Minor
Eastern U.S. region
(847) 854-1666
(adsales@pci.org)

Dick Railton
Western U.S. region
(951) 587-2982
(adsales@pci.org)

PRECAST/PRESTRESSED CONCRETE INSTITUTE

BOARD OF DIRECTORS

Chairman
Robert S. McCormack

Vice Chairman
Robert H. Konoske

Secretary-Treasurer
William F. Simmons III

Millard J. Barney
Craig T. Barrett
Heinrich O. Bonstedt

David G. Buesing
Thomas A. Conroy

Rodney L. Eaves
Harry A. Gleich
Mark N. Groff
C. Hagen Harker
Daniel L. Kennedy

Mark D. Lafferty
Michael W. LaNier
Jason P. Lien
Thomas M. McEvoy
William R. Miller
Donna S. Reuter
John R. Robertson
Robert R. Roeller
Randy Romani
James E. Sorensen
C. Douglas Sutton
James E. Tolson Jr.

Ex-Officio
Thomas J. D'Arcy
Pat Hynes
Kenneth Pensack

TECHNICAL ACTIVITIES COMMITTEE (TAC)

Chairman
Michael W. LaNier

Secretary
Jason J. Krohn

Theresa M. (Tess) Ahlborn
Kenneth C. Baur
Ned M. Cleland
S. K. Ghosh
Harry A. Gleich
Simon Harton
Wayne Kassian
Jason P. Lien

Emily Lorenz
Frank A. Nadeau
Andrew E. N. Osborn
Stephen P. Pessiki
Chuck Prussack
Donald C. Rath
Mario E. Rodríguez
Stephen J. Seguirant
Larbi Sennour
C. Douglas Sutton

**Ex-Officio,
fib Representative**
Thomas J. D'Arcy

PCI STAFF DIRECTORS

President
James G. Toscas

Transportation Systems
John S. Dick

Finance & Administration
Kenneth J. DuPere

Architectural Systems
Industrial Operations & Safety
Sidney Freedman

Research & Education
L.S. (Paul) Johal

Technical Activities
Jason J. Krohn

Education
Kristine McIntosh

Marketing & Communications
Chuck Merydith

Information Systems
Allyn Okun

Controller
Leigh Stevenson

Quality Assurance
John A. Wilke

The *PCI Journal* (ISSN 0887-9672) is published bimonthly by the Precast/Prestressed Concrete Institute, 209 W. Jackson Boulevard, Suite 500, Chicago, IL 60606. Copyright © 2006, Precast/Prestressed Concrete Institute. The Precast/Prestressed Concrete Institute is not responsible for statements made by authors of papers or claims made by advertisers in the *PCI Journal*. Original manuscripts and Reader Comments on published articles accepted on review by the PCI Technical Publications Review Board. No payment is offered. Direct all correspondence to: Editor, *PCI Journal*, 209 W. Jackson Boulevard, Suite 500, Chicago, IL 60606, Tel.: (312) 583-6773, Fax: (312) 786-0353, e-mail: elorenz@pci.org. Advertising Rates: For information, send an e-mail to adsales@pci.org. Subscription Rates: United States \$64 per year, three-year rate \$149. International \$94 per year, three-year rate \$239. Air Mail (additional) \$55 per year. Single/back issue \$12.

POSTMASTER: Please send address changes to *PCI Journal*, 209 W. Jackson Boulevard, Suite 500, Chicago, IL 60606. Periodicals postage rates paid at Chicago and additional mailing offices.